J Physiol 588.21 (2010) pp 4131–4143

The Journal of Physiology

Immunostaining for the α3 isoform of the Na^+/K^+-ATPase is selective for functionally identified muscle spindle afferents *in vivo*

A. Parekh*, A. J. M. Campbell*, L. Djouhri*, X. Fang, S. McMullan, C. Berry, C. Acosta and S. N. Lawson

Department of Physiology and Pharmacology, Medical School, University of Bristol, Bristol BS8 1TD, UK

Muscle spindle afferent (MSA) neurons can show rapid and sustained firing. Immunostaining for the α3 isoform of the Na^+/K^+-ATPase (α3) in some large dorsal root ganglion (DRG) neurons and large intrafusal fibres suggested α3 expression in MSAs (Dobretsov *et al.* 2003), but not whether α3-immunoreactive DRG neuronal somata were exclusively MSAs. We found that neuronal somata with high α3 immunointensity were neurofilament-rich, suggesting they have A-fibres; we therefore focussed on A-fibre neurons to determine the sensory properties of α3-immunoreactive neurons. We examined α3 immunointensity in 78 dye-injected DRG neurons whose conduction velocities and hindlimb sensory receptive fields were determined *in vivo*. A dense perimeter or *ring* of staining in a subpopulation of neurons was clearly overlying the soma membrane and not within satellite cells. Neurons with clear α3 rings ($n = 23$) were all MSAs (types I and II); all MSAs had darkly stained α3 rings, that tended to be darker in MSA1 than MSA2 units. Of 52 non-MSA A-fibre neurons including nociceptive and cutaneous low-threshold mechanoreceptive (LTM) neurons, 50 had no discernable ring, while 2 (Aα/β cutaneous LTMs) had weakly stained rings. Three of three C-nociceptors had no rings. MSAs with strong ring immunostaining also showed the strongest cytoplasmic staining. These findings suggest that α3 ring staining is a selective marker for MSAs. The α3 isoform of the Na^+/K^+-ATPase has previously been shown to be activated by higher Na^+ levels and to have greater affinity for ATP than the α1 isoform (in all DRG neurons). The high α3 levels in MSAs may enable the greater dynamic firing range in MSAs.

(Received 16 July 2010; accepted after revision 27 August 2010; first published online 31 August 2010)
Corresponding author S. N. Lawson: Medical School, Department of Physiology, University Walk, Bristol BS8 1TD, UK. Email: sally.lawson@bristol.ac.uk

Abbreviations CB, Cascade Blue; CV, conduction velocity; DRG, dorsal root ganglion; EB, ethidium bromide; LY, Lucifer yellow; LTM, low-threshold mechanoreceptive; MSA, muscle spindle afferent.

Introduction

Up to 50% of neuronal energy resources are used in supporting Na^+/K^+-ATPase (sodium pump) activity, enabling it to maintain the steep transmembrane Na^+ and K^+ gradients that are necessary for neuronal excitability (Rosenthal & Sick, 1992). The sodium pump exists as a heterodimer of α and β subunits (McDonough *et al.* 1990). The α subunit contains binding sites for ATP, Na^+, K^+ and the cardiac glycoside ouabain, and is central to the pump activity (Sweadner, 1989). In mammalian tissues, four α subunit isoforms (α1–4) and three β subunit isoforms (β1–3) have been identified (Charlemagne *et al.* 1987; Blanco & Mercer, 1998). While the α1β1 isoform is found in nearly every tissue, the α3β1 isoform is principally found in neurons (Blanco & Mercer, 1998) with only 'minor amounts' in skeletal muscle (Clausen, 2003), perhaps consistent with its expression in nerve fibres. The α1β1 and α3β1 combinations have been reported in somatosensory dorsal root ganglion (DRG) neurons (Mata *et al.* 1991).

The α1 isoform of the Na^+/K^+-ATPase a subunit is expressed in 80% of DRG neurons regardless of size (Dobretsov *et al.* 1999). However, high α3 immunoreactivity was non-uniformly expressed (a) within a subpopulation of large-diameter DRG neurons, (b) in intrafusal afferent and efferent nerve fibres and (c) in subpopulations of fibres within sciatic and peroneal nerves

*A. Parekh, A. J. M. Campbell and L. Djouhri contributed equally to this study and should be considered co-first authors.

DOI: 10.1113/jphysiol.2010.196386

that innervate both skeletal muscle and skin but not in sural and saphenous nerves projecting almost exclusively to skin (Dobretsov *et al.* 2003). These findings suggested that the $\alpha 3$ Na^+/K^+-ATPase is expressed in muscle spindle afferent (MSA) fibres but not other somatosensory fibres. However, other types of primary afferent, e.g. cutaneous $A\alpha/\beta$ low-threshold mechanoreceptors (LTMs) and $A\alpha/\beta$ nociceptors have some overlap of sizes and conduction velocities (CVs) with MSAs (Fang *et al.* 2005*b* and Djouhri L., Fang X., Gao L. and Lawson S.N., unpublished observations). Therefore, direct functional studies of different somatosensory afferent types were needed to determine whether $\alpha 3$ Na^+/K^+-ATPase is expressed exclusively or preferentially in MSAs, and if so, whether it is expressed equally in MSA subtypes. We found high $\alpha 3$ immunointensity exclusively in neurons labelled with the antibody RT97 (against highly phosphorylated epitopes on 200 kD neurofilament subunits), which in rat labels DRG neuronal somata with myelinated fibres (Lawson & Waddell, 1991). We therefore subsequently focussed mainly on $\alpha 3$ immunoreactivity in A-fibre neurons.

Physiological identification of sensory receptive properties and conduction velocity measurements were made *in vivo* in individual rat DRG neurons with intracellular recording with dye-filled electrodes. Intracellular dye injection enabled subsequent $\alpha 3$ immunocytochemistry on the dye-injected identified neurons to be made and correlated with sensory properties in individual neurons. A few identified guinea pig DRG neurons were similarly examined to determine whether patterns in rat occur in other species.

Methods

Animal preparation

All procedures were performed under a licence held according under the provisions of the Animals (Scientific Procedures) Act 1986, reviewed by the University of Bristol Ethical Review Group.

These experiments also comply with *The Journal of Physiology* policy and UK regulations on animal experimentation described by Drummond (2009).

The main study was on young female Wistar rats (6–7 weeks of age, 150–180g); smaller numbers of neurons were recorded in young female Dunkin–Hartley guinea pigs (160–275g). Methods described apply to both species unless otherwise indicated. For detailed guinea pig methods see Djouhri *et al.* (1998).

Animals were deeply anaesthetised to areflexia with sodium pentobarbitone (50–70 mg kg^{-1} I.P.). A tracheotomy enabled artificial ventilation. The left carotid artery and external jugular vein were cannulated to, respectively, enable blood pressure monitoring and allow supplementary anaesthetic (I.V., 10 mg kg^{-1} approximately hourly); this dosage regime causes sustained deep anaesthesia. A laminectomy exposed L3–L6 DRGs (rats) or L5–S1 DRGs (guinea pigs) and their dorsal roots. Details of the recording set-up have been published (Lawson *et al.* 1997; Fang *et al.* 2002). Briefly, dental impression material (Xantopren VL plus, Hanau, Germany) was used to create a liquid paraffin pool maintained at ∼30°C (range 28.5–33.5°C). Immediately prior to recording, the dorsal root of the DRG under study was cut close to its entry to the spinal cord and placed over a pair of platinum stimulating electrodes in the paraffin pool. A small silver wire platform beneath the DRG separated it from underlying tissues to improve recording stability.

The hind limb was extended and the dorsal surface of the foot was glued with cyanoacrylate glue to a platform beneath it with the plantar surface of the foot upwards. This increased recording stability, but also stretched the leg muscles.

Just before electrophysiological recording, muscle relaxant (pancuronium, 0.5 mg kg^{-1} I.V. or gallamine triethiodide, Flaxedil, 2 mg kg^{-1} I.V.) was administered accompanied by further anaesthetic (sodium pentobarbitone, 10 mg kg^{-1} I.V.). Muscle relaxant was given at approximately hourly intervals, always with further (10 mg kg^{-1} I.V.) anaesthetic. The animal was artificially ventilated and end-tidal CO_2 monitored. Blood pressure remained stable indicating deep anaesthesia throughout the experiment. In both species, the level of anaesthetic was maintained at that which kept the animal deeply anaesthetised and areflexic during the 2–3 h of surgery prior to administration of muscle relaxant. Our experience of using this anaesthetic regime (frequency and dose) in the absence of muscle relaxant for the whole duration of similar experiments shows that it maintains deep anaesthesia and areflexia throughout.

Electrophysiological recordings

Intracellular recordings were made using glass microelectrodes filled with one of three fluorescent dyes. These were Lucifer yellow CH (LY; Sigma, St Louis, MO, USA; 5 mg ml^{-1} in 0.1 M LiCl), ethidium bromide (EB; Sigma; 2.5–6 mg ml^{-1} in 1 M KCl) or Cascade Blue (CB; Molecular Probes, Eugene, OR, USA; 3% in 0.1 M LiCl). Electrode impedence ranged from 200 to 500 mΩ for LY and CB, and 80 to 120 mΩ for EB. In rat, neurons were mostly in L5 DRG (65) with some in L4 (11) DRG, 1 in L6 and 1 in L3. In guinea pig, neurons were mainly (12) in L6, with 1 in L5 and 5 in S1. The microelectrode was advanced into the DRG until a membrane potential (V_m) was detected. The dorsal root was then stimulated with a rectangular pulse (0.03 ms for A- and 0.3 ms for C-fibre neurons) at

a voltage up to twice threshold for A- and 1 to 1.5 times threshold for C-fibre units.

Conduction velocity (CV). For each neuron, CV was calculated as previously described (Djouhri & Lawson, 2001) from the time (latency) between dorsal root stimulation and the onset of the evoked somatic AP, and distance (usually 4–14 mm) between the stimulating electrode (cathode) and the neuronal soma position in the DRG (error ± 0.25 mm). This method includes utilization time and thus underestimates CV (see below). Each neuron was classified by its CV, according to CV boundaries determined previously (also including utilization time) from dorsal root compound action potentials in rats (Fang *et al.* 2002), and guinea pigs (Djouhri & Lawson, 2001) of the same age and weight as those used here. CV boundaries were: for rats C, <0.8 m s^{-1}; for Aδ, 1.5–6.5 m s^{-1}; and Aα/β, >6.5 m s^{-1}: and for guinea pig, C, <1.1 m s^{-1}; Aδ, 1.1–4.2 m s^{-1}; and Aα/β, >4.2 m s^{-1}. For explanation and discussion of these values see Djouhri & Lawson (2001 and Fang *et al.* (2002). The latencies include utilisation time, the time taken for the stimulus to evoke an action potential, as well as conduction time. This greater latency would cause an underestimate especially of the faster CVs (Aα/β) (Waddell *et al.* 1989); in addition, the shortest latencies could not be accurately measured in the shortest nerves due to overlap of the stimulus artefact with the AP onset. Although muscle afferent CVs are normally classified as groups I, II, III and IV, because this study includes cutaneous afferents we use the Greek notation throughout, that is, respectively: Aα, Aβ, Aδ and C CV groups, with Aα and Aβ grouped as Aα/β.

Ongoing firing. Before searching for the receptive field, the presence of any ongoing firing was recorded, for 1–2 min.

Identification of sensory receptive properties

Low-threshold mechanoreceptive neurons (LTMs). Hand-held stimulators were applied to the left hindlimb and flank (see Lawson *et al.* 1997 and Fang *et al.* 2002). LTMs responded to light brushing (soft brush), light tapping, gentle pressure with blunt objects and calibrated Von Frey hairs. Aα/β LTMs included muscle spindle afferent (MSA) units and cutaneous units (see below). A brief application of ethyl chloride or ice to the receptive field was used as a cooling stimulus because some LTMs (including C LTMs, D hair units and slowly adapting type II units, see Lawson, 2005) also respond to cooling.

Muscle spindle afferent (MSA) LTM units. Most showed ongoing firing, the rate of which was very sensitive to light pressure applied over the entire body of the muscle; they often responded to vibration (e.g. tuning fork at 100 Hz). If the receptive field did not move with the skin when the skin was moved, a cutaneous receptive field was excluded. The continuous stretch of the hind limb stretches especially flexor muscles. The ongoing firing can be explained by the muscle relaxant causing relaxation of extrafusal muscles, enhancing passive stretching of the muscle spindles. This would unload the Golgi tendon organs. Because of this, Golgi tendon organ afferents were unlikely to be stretched enough to be activated even when pressure or vibratory stimuli were applied; they are therefore unlikely to be included in this study. We therefore classed Aα/β units that had ongoing firing and subcutaneous receptive fields, and/or that showed altered firing in response to pressure on the muscle, as MSAs. MSAs are often subdivided into group Ia afferents with primary endings or group II afferents with secondary endings (Boyd, 1962; Matthews, 1964). Group Ia afferents respond to stretch with an initial phasic discharge followed by a static discharge, and respond well to vibration of 100 Hz, whereas group II afferents respond to stretch with a predominantly static discharge pattern and respond poorly to such vibration, as do Golgi tendon organs (Matthews, 1964, 1984; Brown *et al.* 1967). In the present study, some MSAs were clearly more dynamic and others more static in their responses. A post hoc subdivision into MSA1 (1a) or MSA2 (group II) units was made on the basis of the greater adaptation to gentle sustained pressure, greater sensitivity to rapid movement of stimuli, and greater ability to follow a 100 Hz vibratory stimulus of MSA1 *versus* MSA2 units (Matthews, 1964, 1984; Brown *et al.* 1967). MSA2 units adapted more slowly, were less responsive to vibration or gentle tap and responded well to static or slowly moving stimuli. Some MSAs were not characterized precisely enough for inclusion in either category.

Cutaneous LTM units. These responded to low-intensity mechanical skin stimulation. Their receptive fields moved with the skin when that was moved relative to the underlying tissues. Those with Aα/β fibres included guard hair follicle (G hair) afferents responding to movement of one or more hairs while F (field) units responded to skin contact or movement of many hairs; both G hair and field units were rapidly to moderately rapidly adapting. G hair and field units were combined as G hair/field (G/F) units throughout (see Djouhri *et al.* 1998; Fang *et al.* 2002). Aα/β cutaneous LTMs also included rapidly adapting (RA) units that responded to rapid movement of low-intensity mechanical stimuli across glabrous skin. Pacinian corpuscle afferents (very rapidly adapting Aα/β LTMs responding to light tap or vibration) were not included in this study. Aα/β slowly adapting (SA) LTMs responded with a sustained discharge to static cutaneous pressure. Aδ down hair (D hair) LTMs were highly sensitive

to slow movements of hair with a brush, to skin stretch and cooling.

Nociceptive units. Neurons that showed no response to non-noxious stimuli were tested with noxious stimuli that were painful if applied to thin human skin. Noxious mechanical stimuli were applied with needle, forceps (fine and/or toothed) or coarse flat forceps; noxious thermal stimuli were cooling by a brief localized spray of ethyl chloride and/or heating with water at a temperature of $>50^{\circ}$C. Neurons that responded only, or with a much greater response, to noxious stimuli were classed as nociceptors. Nociceptors included high-threshold mechanoreceptors (HTMs), polymodal, mechano-heat units and mechano-cold units (see below for properties).

One C-fibre unit was unresponsive to both noxious and non-noxious stimuli. C unresponsive neurons have immunocytochemical properties that are similar in many respects to C-nociceptors (Djouhri *et al.* 2003; Lawson, 2005; Fang *et al.* 2006), and because this had an AP shape similar to C-nociceptors it was classed with the C-nociceptor class, as a nociceptor-type unit. No C-fibre units sensitive only to warm, heat, cooling or cold were included in the present study.

Fluorescent dye injection

After sensory characterization and recording were complete, fluorescent dye was injected into the soma with regular current pulses (1 nA, max 1.3 nA for 500 ms at 1 Hz for 10–15 min for A-fibres and 6–10 min for C fibres); negative current was passed to eject LY and CB and positive for EB dye (Lawson *et al.* 1997; Fang *et al.* 2002). Receptive field properties and conduction latency were rechecked to ensure the electrode tip had remained in the same neuron.

Records were kept of locations of all electrode tracks, and of numbers and depths of all neurons penetrated in each track, and noting those that were dye-injected. A maximum of three LY injections (central, mid and peripheral in the DRG) were made in the longer (2 mm) L5 rat DRGs, and two in other DRGs (for more detail see Fang *et al.* 2002).

Tissue preparation and finding dye-injected neurons

The animal was perfused through the heart with 0.9% saline followed by Zamboni's fixative following an anaesthetic overdose. DRGs were removed and the conduction distance measured. The DRG was post-fixed by immersion in Zamboni's for 1 h and left overnight in 30% sucrose buffer at 4°C. Serial 7 μm cryostat sections of DRGs were made, and once mounted onto slides, each section was examined under a fluorescence microscope (Leica DMRBE, Leica Microsystems UK Ltd, Milton Keynes, UK) for the dye-filled neurons. Their locations were compared with the records made during experiments and if the position, depth or number of dye-labelled neurons did not match experimental records, or if the dye fluorescence intensity was weak, neurons were rejected. This avoided inclusion of neurons labelled by dye leakage rather than current ejection (Lawson *et al.* 1997). Locations of every successfully dye-labelled neuron within each section was recorded with camera lucida drawings and images captured with a CCD camera (Hamamatsu, Hamamatsu City, Japan). Tissue sections were stored at -20°C until immunocytochemistry was performed.

Tissue preparation for α3 and RT97 co-localisation. Four female rats (weight approximately 170 g) were fixed by perfusion as described earlier, and the L4 DRGs were post-fixed for 1 h and left overnight in 30% sucrose buffer and then 7 μm cryostat sections were taken transversely at 400 μm intervals throughout each DRG, giving a series of between four and six equally spaced sections for each DRG.

Immunocytochemistry

Two types of immunocytochemistry were carried out. Fluorescence immunocytochemistry was used to examine α3 co-localisation with neurofilaments on DRGs from which recordings had not been made. Avidin–biotin complex (ABC) immunocytochemistry was carried out to determine the α3 immunoreactivity of (a) individual dye-injected identified neurons and (b) comparison of α3 and HCN1 immunoreactivity on adjacent sections of neurons DRGs in which recordings had not been made.

Antibodies. The primary antibody against α3 Na^+/K^+-ATPase was a rabbit polyclonal (TED, used at 1:500–1:2000 for fluorescence immunocytochemistry and 1:8000 for ABC immunocytochemistry) was a gift from Dr Thomas Pressley. Its specificity for α3 was characterised with Western blot (Pressley, 1992; Juhaszova & Blaustein, 1997). Its staining patterns have been shown to be the same as with a different rabbit polyclonal antiserum raised against rat Na^+/K^+-ATPase α3 subunit fusion protein (Upstate Biotechnology, Lake Placid, NY, USA), and a monoclonal anti-α3 antibody IgG1 (Clone XVIF9-G10, Mα3-915, Affinity Bioreagents Inc., Golden, CO, USA) (Dobretsov *et al.* 2003).

The anti-HCN1 rabbit polyclonal antibody was from Alomone Labs Ltd, Jerusalem, Israel, raised against peptides 6–24 of rat HCN1. It had previously been characterised against HCN1 selectively expressed in heterologous cells and in Western blots (Han *et al.* 2002; Chaplan *et al.* 2003; Much *et al.* 2003; Notomi *et al.* 2004; Peters *et al.* 2009).

The RT97 antibody (used at 1:4000, a gift from J. N. Wood) was previously characterised (Wood & Anderton, 1981; Calvert & Anderton, 1982) and binds to a highly phosphorylated epitope on the 200 kD neurofilament subunit. It labels the population of large, light neurons in DRGs (Lawson *et al.* 1984) that have A-fibres (Lawson & Waddell, 1991). Secondary antibody for ABC immunocytochemistry for both α3 *and* HCN1 was biotinylated anti-rabbit IgG, (1:200, from Vector Laboratories, Peterborough, UK). Secondary antibodies for fluorescence immunocytochemistry were from Molecular Probes. They were: for RT97, Alexa Fluor 488 goat anti-mouse IgG (1:400) and for TED, (anti-α3) Alexa Fluor 594 goat anti-rabbit IgG (1:600). See Supplementary Fig. S1 and legend for details.

ABC immunocytochemistry. This was carried out as previously described in detail (Fang *et al.* 2002). Briefly, after block of endogenous peroxidase and biotin-like activity with 3% H_2O_2 and an avidin–biotin kit (Vector Laboratories, Peterborough, UK), respectively, sections were incubated with primary antibody for 48 h at 4°C. After washing, sections were incubated for 30 min at room temperature with biotinylated secondary antibody. Avidin–biotin complex (ABC) staining was performed using the Vectorstain Elite avidin–biotin Kit followed by incubation in diamino-benzidene. Omission of primary antibody resulted in no staining.

Immunofluorescence. Fluorescence immunocytochemistry was carried out as follows. Following a blocking stage with 10% fetal calf serum (FCS) and 1% normal goat serum (NGS), in 0.1 M PBS (phosphate-buffered saline) for 30 min, primary antibodies were added in 10% FCS, 1% NGS and 0.05% Triton-X 100 in 0.1 M PBS and incubated overnight at 4°C. After washing with PBS, sections were incubated in 1% NGS in PBS, and then secondary antibody was applied in 0.1 M PBS plus 1% NGS for 30 min at room temp. After washing, slides were mounted in Vectashield. Again, omission of the primary antibody resulted in no detectable staining. Using epifluorescence microscopy (×40 objective) and appropriate filters (Omega filters, Brattleboro, USA), counts were made of all neuronal profiles with clear nuclei and with clear α3-immunoreactive rings around the perimeters of neurons in five sections of an L4 DRG from each of four rats. Whether each neuron with a clear α3 ring was RT97 positive or negative was recorded.

α3 immuno-staining pattern. With both ABC and fluorescence immunocytochemistry, neurons with ring staining and more intense cytoplasmic staining were a subpopulation of large-diameter neurons (Fig. 1) as previously described (Dobretsov *et al.* 1999).

Dye-injected neurons: analysis of immunointensity

Subjective assessment of α3 ring staining. Subjective intensity of α3 ring staining in injected neurons was determined relative to other neurons in the same section, on a scale of 0–5 where 0 was negative (no ring visible), 1 = just visible faint positive ring; 5 = the most intensely stained ring in the section. The subjective ring intensity for each neuron was the average of estimates by two pairs of observers.

Image analysis of pixel densities. The semi-quantitative image analysis methods previously used to determine relative immunocytochemical intensities of cytoplasmic staining (Fang *et al.* 2002, 2005*a*; Djouhri *et al.* 2003) were adapted to the analysis of both cytoplasm and ring α3 immunostaining as follows. Digital images of each dye-injected neuron were captured under a ×40 objective, plus images of the three most intensely stained neurons in the same section and three most weakly stained neurons in the vicinity of the dye-injected neuron (Fang *et al.* 2002). The pixel density of immunostaining for α3 was measured with image analysis software (Simple PCI, Digital Pixel, Brighton, UK) for both ring and cytoplasmic staining in each of the above neurons. The α3 ring pixel density was the average pixel density under three lines drawn within the most darkly stained regions of the ring. The cytoplasmic density was the average density over the neuronal cytoplasm (excluding the nucleus). The three most negative neurons were those with weakest cytoplasmic staining and no defined ring staining, thus only their cytoplasmic pixel density was measured.

Relative intensity of α3 staining. The relative α3 staining intensities of each dye-injected neuron were determined by comparison with neuronal staining in the same section. For each dye-injected neuron, the 0% value for the section was the mean cytoplasmic pixel density of the three most weakly stained neurons or of the dye-injected cell if that was the most weakly stained in the section (a). The 100% level for the ring (c) staining was the mean pixel density of the three neurons with the most strongly staining rings in the section or of the dye-injected neuron if that was the strongest ring staining. Cytoplasm and ring staining of the injected neuron provided the values d and e, respectively. Therefore, relative intensities for ring and cytoplasm of the injected neuron were calculated as a percentage of the maximum ring intensity, calculated as $100 \times (e - a/c - a)$ for the ring, and $100 \times (d - a/c - a)$ for the cytoplasm. For both ring and cytoplasm staining, the word 'intensity' hereafter means percentage intensity relative to maximum

(100%) ring intensity and minimum (0%) cytoplasmic intensity calculated as above. This method results in a dye-injected neurons that is the most intensely stained in the section having a relative intensity of >100%. These were rounded down to 100%.

This method is semi-quantitative enabling relative intensities of injected neurons to be compared and minimising effects of staining variability between sections (Lawson *et al.* 1997; Fang *et al.* 2002). Although for clarity of expression we use the terms $\alpha 3$ positive and $\alpha 3$ negative (>40% and <40% relative ring staining intensity, respectively; see Results), some '$\alpha 3$ negative' neurons may express low, possibly functional, levels of the $\alpha 3$ subunit.

$\alpha 3$ and neuronal size. Cross-sectional areas of dye-injected neurons were measured with the image analysis system in neurons for which the cross sectional area of the largest section was available. This estimate of cell size does not take into account possible non-spherical (elongated or flattened) shapes of some DRG neurons. It was plotted against $\alpha 3$ ring relative intensity (above).

$\alpha 3$ co-localisation with RT97. Four female rats (~170 g) were fixed and the L4 DRGs were treated as described earlier and 7 μm transverse cryostat sections were taken at 400 μm intervals, giving a series of four to six equally spaced sections for each DRG. After fluorescence immunocytochemistry (see above), epifluorescence microscopy (×40 objective) and appropriate filters (Omega filters, Brattleboro, USA), were used to make counts of all neuronal profiles with clear nuclei and with clear $\alpha 3$ immunoreactive rings around the perimeters of neurons in the L4 DRG from each rat. Whether each neuron with a clear $\alpha 3$ ring was RT97 positive or negative was recorded.

Statistical analyses

Data were analysed using Prism 4 and 5 software (GraphPad software, Inc., San Diego, CA, USA). Following ABC immunocytochemistry, the small numbers in some neuronal subcategories necessitated the use of non-parametric statistics to compare median values (Kruskal–Wallis test for multiple comparisons and Mann–Whitney tests for comparisons between two medians).

Results

Strong staining around the perimeter of a subpopulation of the large-diameter neurons was seen; we call this the 'ring' staining. This $\alpha 3$ ring staining is over the DRG neuron membrane: as can be seen in Fig. 1*A* the satellite cell sheath shown by arrows is devoid of the staining, suggesting that it is associated with the neuronal membrane. This view is supported by $\alpha 3$ staining over the fibre perimeter inside some of the myelin sheath (e.g. in Fig. 1*F*), and the above-background evenly stained cytoplasm in neurons with ring staining, suggesting both are within the same neuron. The $\alpha 3$ 'ring' immunoreactivity was similar with ABC or immunofluorescence (Fig. 1*B* and *D*). Within the cytoplasm of these $\alpha 3$ ring positive neurons there is also elevated staining.

$\alpha 3$ and neurofilament co-localisation

All 218 (100%) neuronal profiles with visible nuclei and clear $\alpha 3$ rings were neurofilament-rich i.e. RT97 positive but not all neurofilament-rich neurons had $\alpha 3$ ring staining (see Fig. 1*B* and *C*, and Supplementary Fig. S1 for colour). As neurofilament-rich DRG somata in rat have A-fibres (Lawson & Waddell, 1991), this suggests that DRG neurons with clear $\alpha 3$ rings all have A-fibres. We therefore targeted A-fibre neurons in the present study but included a few C-fibre neurons for comparison.

$\alpha 3$ and HCN1 staining

We see ring staining that initially looks to be of a similar nature with an antibody against HCN1 (one of the isoforms of the channel underlying the I_h current). To ensure that these antibodies were not labelling the same proteins, we examined whether $\alpha 3$ and HCN1 rings were visible in the same neurons, on adjacent 7 μm sections, as a further check to ensure that they could not be staining the same protein. Figure 1*E* shows ~12 clear HCN1 ring positive neurons, but only two of these have clear $\alpha 3$ rings (Fig. 1*D*). In Fig. 1*F* and *G* a neuron with clear HCN1 and $\alpha 3$ ring staining is shown; note that a subpopulation of myelinated fibres perimeters is stained for $\alpha 3$ but not for HCN1 (arrows). Thus, although the ring staining is similar, the overall staining pattern for the two antibodies are clearly different, supporting the specificity of the staining obtained with the $\alpha 3$ antibody.

$\alpha 3$ and sensory properties in dye-injected neurons

Representative examples of dye-injected and $\alpha 3$-immunostained identified neurons are shown in Fig. 2. Three $\alpha 3$ negative neurons (rat) with no visible ring staining on the left (*A–C*) are a C-nociceptor type, an Aα/β RA and an Aα/β nociceptive afferent. Three MSA neurons (right, *D–F*) in rat and guinea pig all showed clear $\alpha 3$ ring staining. Note the sections through MSAs in Fig. 2*A–F* are not through the nucleus and thus do not represent the full size of the MSAs. For approximate sizes of MSAs see Fig. 4*B* and *C*.

Subjective *versus* objective α3 intensities. The subjective judged and objectively calculated relative intensities for α3 ring immunostaining were highly significantly linearly correlated (Fig. 2*G*), indicating that the objectively values reflect the subjective appearance of the rings. The dotted vertical line from the *X*-axis value representing a clearly visible ring (a subjective score of $\geq$1) intersects the linear regression line at 40% relative intensity. Any ring intensity >40% was therefore classed as positive. Cells with values below this may have α3 immunostaining, but their ring staining was not distinguishable from cytoplasmic staining.

Identified neurons included in the study. A total of 78 neurons with identified sensory properties were successfully labelled and immunostained to show α3 immunoreactivity in rat DRGs. They included 45 LY,

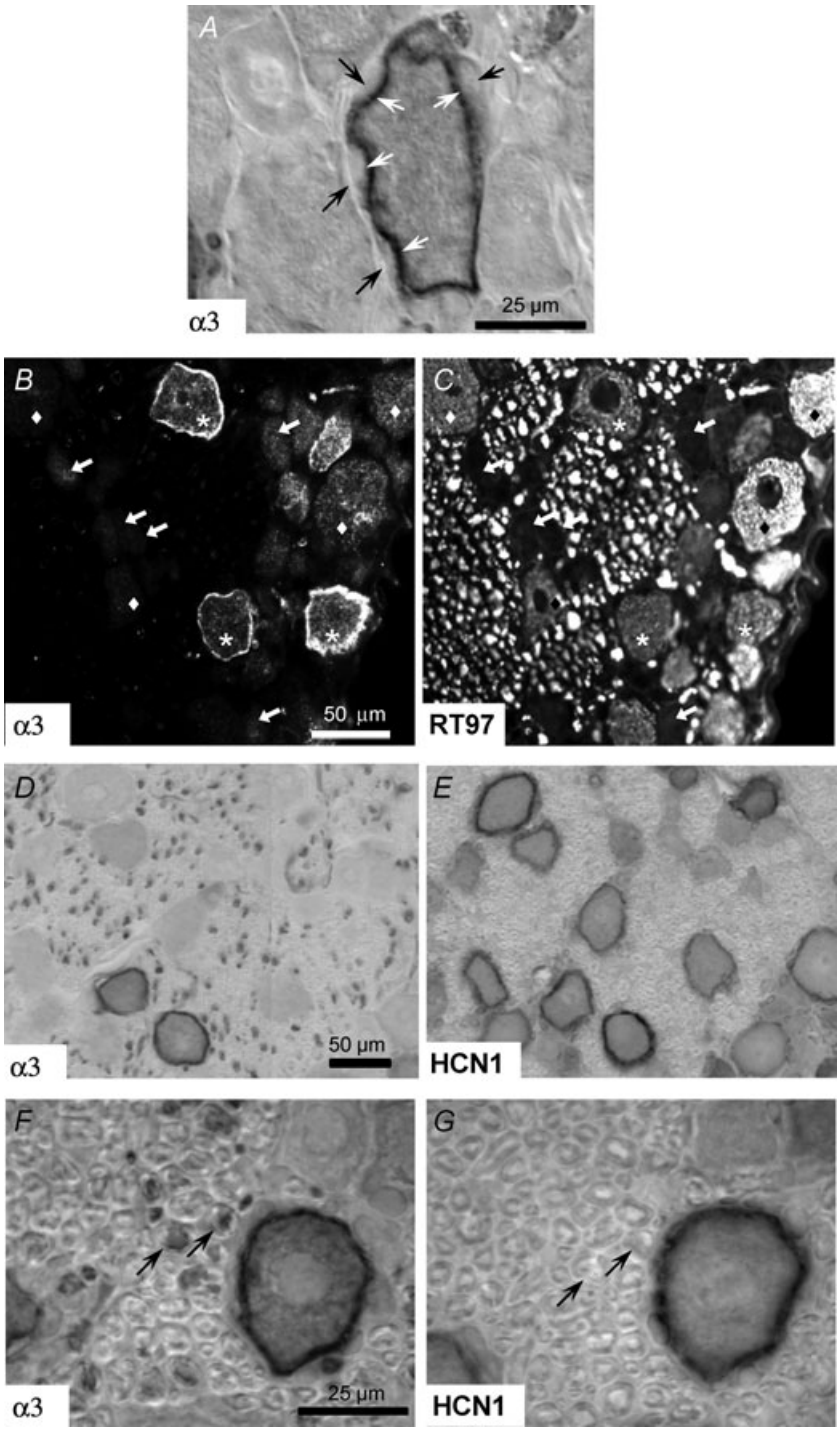

Figure 1. α3 co-localisation with neurofilament and HCN1
A, high power (×100 objective) view of a neuron with a clear α3 stained ring. Arrows indicate satellite cells around the neuron that are not labelled, showing that the ring must be over the neuronal perimeter/membrane. *B* and *C*, double labelling immunofluorescence of rat DRG neurons with α3 (*B*) and RT97 (*C*) immunostaining illustrates that neurons with α3 rings are neurofilament rich (using the antibody RT97). Diamonds (white in *B* and black in *C*): RT97 positive (neurofilament rich) but α3 negative; asterisks: α3-positive neurons are neurofilament rich; small arrows: RT97-negative neurons appear black, none is α3 positive. *D* and *E*, adjacent sections containing the same neurons were immunostained (ABC method) for α3 (*D*) and HCN1 (*E*). In the same field two neurons had clear α3-positive rings, but ~12 showed HCN1 ring staining. A higher power view of a neuron stained for both is shown in *F* (α3) and *G* (HCN1). Clearly, fibres within myelinated sheaths were stained for α3 (*D* and *F*) but not HCN1 (*E* and *G*). Scale bars in *B*, *D* and *F* also relate to *C*, *E* and *G*,respectively.

4 CB and 29 EB dye-injected neurons. They were classified as 56 LTMs (5Aδ and 51 Aα/β) and 22 nociceptors (3C, 6Aδ and 13Aα/β). A total of 14 neurons in guinea pig DRG (6 LY, 2 CB and 6 EB) were also successfully examined (for numbers in each group see Fig. 2).

Subjective ring staining ratings. All 23 MSA units in rat DRGs showed clear rings (subjective rating $\geq$1) and had a ring intensity $\geq$40% (see Fig. 3*A* and *B*). One G hair unit and one cutaneous RA unit had weakly positive rings (subjective rating of 1, but both just $<$40% intensity). All

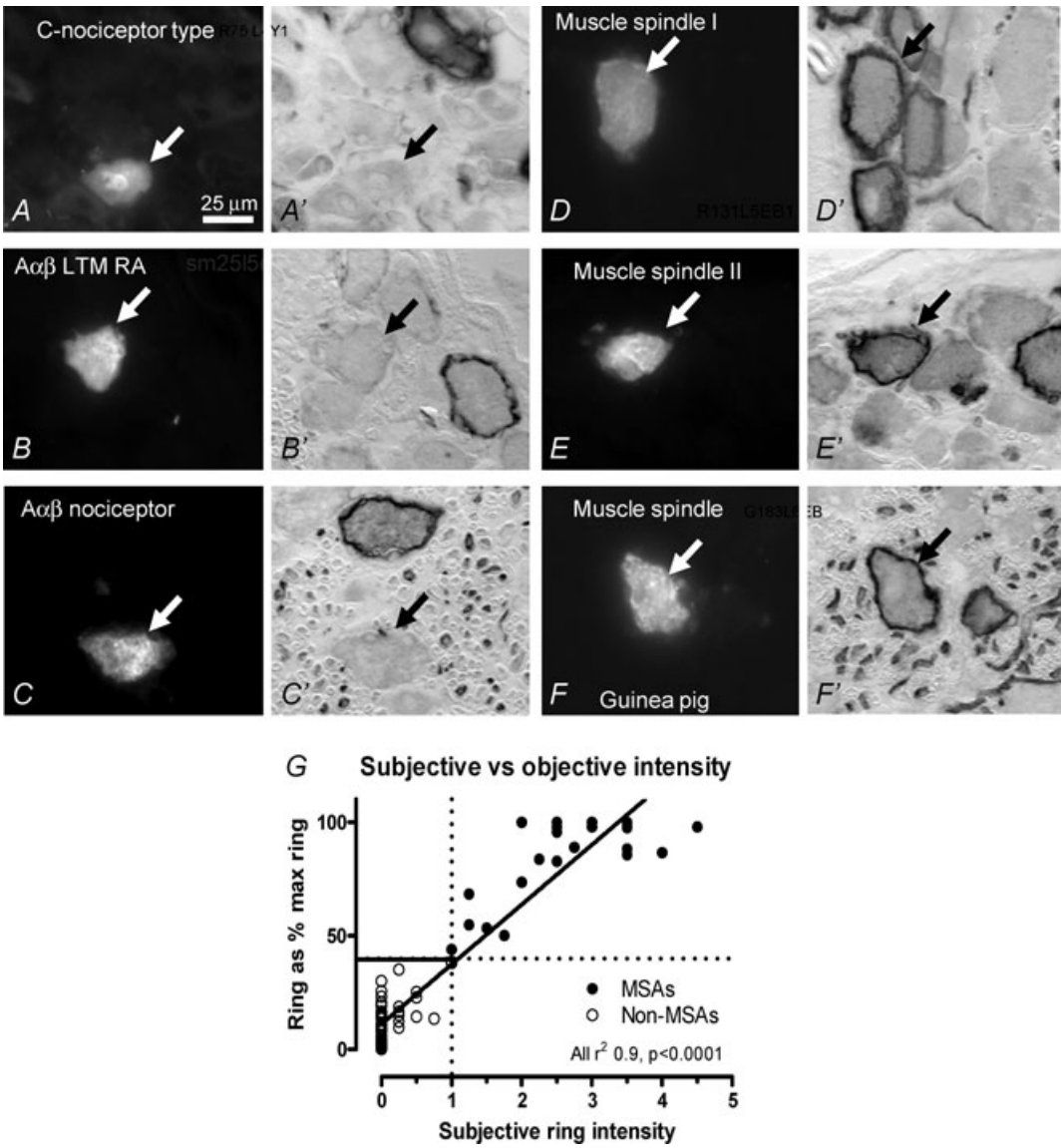

Figure 2. α3 immunoreactivity in dye-injected identified DRG neurons
A–F, the left hand image in each case shows dye fluorescence in a section through the neuron (arrow) that was characterised *in vivo*. The right hand image is of the same neuronal section (arrow) after ABC immunocytochemistry for α3 (dark reaction product) (*A′–F′*). There is no visible α3 ring in *A–C*; *A*: a C-fibre nociceptive type (unresponsive) neuron. *B*: an Aα/β RA neuron; *C*: an Aα/β nociceptor. *D*, *E* and *F* are neurons with clearly positive α3 rings over the perimeter of the neuron; all are MSAs. They are: *D*, a type I MSA; *E*, a type II MSA; and *F*, a guinea pig MSA. Apart from *F*, all neurons are from rat. The only dye-labelled profile with a clear nucleus is the C-fibre neuron; the other profiles are not through the middle of the neuron and thus do not show the full neuronal size. The 25 μm scale bar in *A* applies to all images from *A–F*. *G*, correlation of subjective *versus* objective relative intensities of dye-injected neurons. *Y* axis: ring relative intensity for α3 staining the dye-injected neurons in relation to maximum ring staining in that section; *X* axis, subjective judgement for the same dye-injected neuron, judged relative to the maximum ring intensity within that section. The correlation is highly significant. Neurons judged as having a clear α3 ring stain (scores 1–5) all had an α3 ring relative staining intensity of $\geq$40%.

other units were classed as having no discernible rings and had intensities over the perimeter of the cell (also called ring intensities) of <40%.

Image analysis

$\alpha 3$ ring staining intensity. Staining intensity determined with image analysis showed that in rat, the median ring intensity was 90% for MSAs, much greater than for any other group (medians for other groups ranged from 8.5 to 20% Fig. 3*B*). In fact, all non-MSA neurons had ring intensity <40% which means they are classed as negatively stained and are probably expressing only low levels of $\alpha 3$. A Kruskall–Wallis test between all groups with Dunns *post hoc* test between all pairs of groups showed a significant difference between the MSA median and that of each of the other groups except SA; P values for these differences with the MSA median were $P < 0.05$ for C nociceptors and D hair units, and $P < 0.0001$ for Aα/β nociceptors, G/F (G hair/field) units and $P > 0.001$ for RA units. A Mann–Whitney test between MSAs and SAs was also significant ($P = 0.0002$). Since there was no significant difference between $\alpha 3$ ring medians of any of the non-MSA groups, they were combined; a Mann–Whitney test between all non-MSAs and MSAs was highly significant ($P < 0.0001$, see Fig. 3*B*). Thus, median $\alpha 3$ ring intensity was significantly higher for MSAs than for any other group of neurons examined.

In guinea pig, despite the small numbers of units examined, DRG neurons showed similar patterns relative to sensory properties to those in rat. Again, the MSAs showed significantly more intense $\alpha 3$ ring staining than the non-MSA units taken together ($P < 0.001$) (Fig. 3*C*) as in rats. The staining pattern of MSAs is also similar to that in the rat (see $\alpha 3$ staining in a guinea pig MSA and in rat MSAs in Fig. 3).

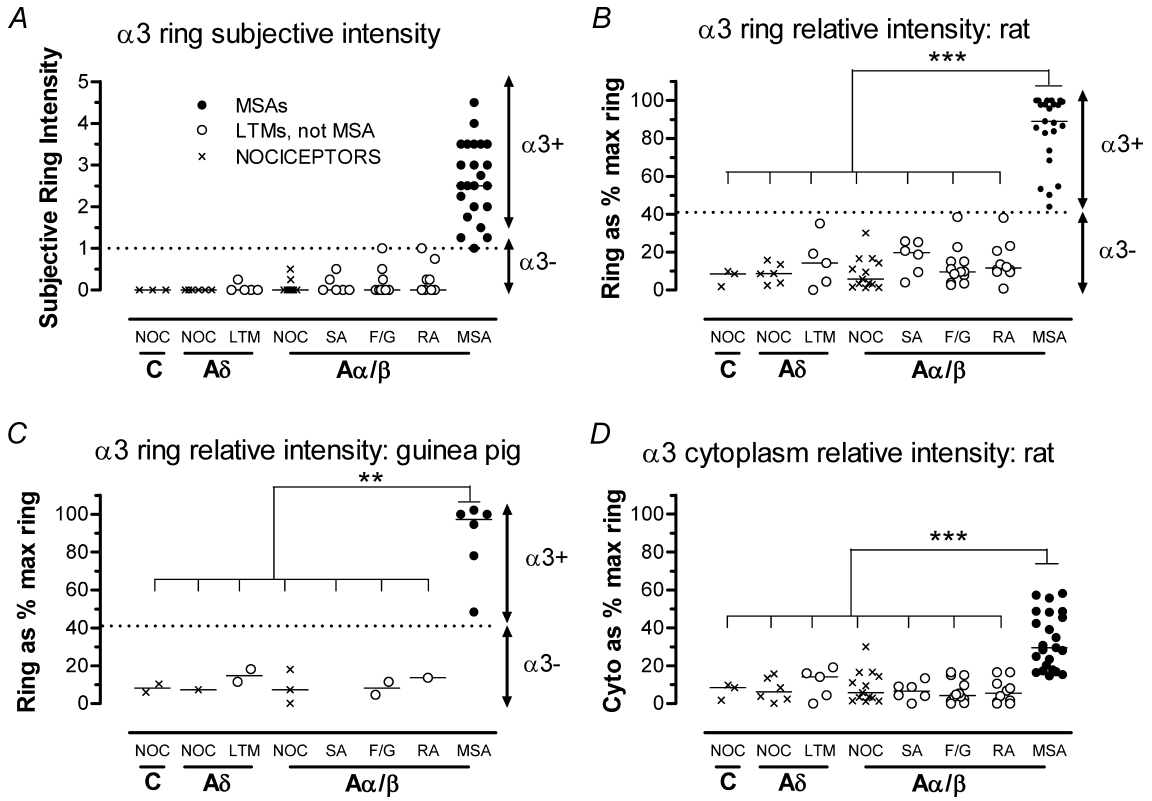

Figure 3. $\alpha 3$ immunointensity in relation to sensory properties
Scatter plots for DRG neurons of all CVs with identified sensory properties are shown. *A*, subjective judgements of $\alpha 3$ ring relative intensity plotted for single dye-injected DRG neurons with different sensory receptive properties in the rat. 1–5 have clearly visible rings, 5 is the darkest ring staining in the section. *B–D*, $\alpha 3$ relative immunointensities measured with image analysis (see Methods) for the same neurons as in *A*. *B*, rat $\alpha 3$ ring relative intensity. MSAs are positive (≥40% $\alpha 3$ ring intensity) and all other types of neurons are negative (<40% maximum ring intensity). *C*, guinea pig $\alpha 3$ ring intensities show similar patterns for $\alpha 3$ ring relative intensity that, despite the small n values, are consistent with the patterns in rat (*B*), with MSAs having a clearly positive (>40%) $\alpha 3$ ring. *D*, rat $\alpha 3$ cytoplasmic intensity against sensory properties. The median cytoplasmic relative intensity is significantly greater in MSAs than in other types of neuron but in contrast to ring intensities (*B*) there is some overlap of relative cytoplasmic intensities between a few MSAs and other units. Asterisks denote level of significance as follows: $^*P < 0.05$, $^{**}P < 0.01$, $^{***}P < 0.001$.

Cytoplasmic α3 staining intensity. In rat DRG neurons, the median cytoplasmic α3 intensity (relative to maximum ring intensity in the section) was also higher for MSA units (median 32%) compared with that of any other group (range of medians 4.8–11.7%; see Fig. 3*D*). Comparing all groups, with Dunn's *post hoc* test between all groups, the median staining for MSAs was significantly higher than for F/G units, RA units, Aα/β nociceptors ($P < 0.001$ in each case) and Aδ nociceptors ($P < 0.01$). MSA and SA medians were also highly significantly different ($P < 0.01$, Mann–Whitney). There was no difference between medians of any non-MSA group. These were therefore combined and a Mann–Whitney test showed the medians of all non-MSAs combined to be highly significantly different ($P < 0.0001$) from MSAs.

α3 ring *versus* cytoplasmic staining. Both the α3 ring and cytoplasmic intensities were greater in MSAs than any other unit examined in rat. Relative intensities of cytoplasm and ring staining for the dye-injected neurons were positively correlated significantly for MSAs ($P < 0.05$) and highly significantly ($P < 0.0001$) for all other units together (Fig. 4*A*) and also for these other units subdivided into nociceptors ($P < 0.0001$, $r^2 = 0.7$) and LTMs ($P < 0.0001$, $r^2 = 0.6$). The slopes of the regression lines (shown) for MSA and all non-MSA units were not significantly different but their elevations were highly significantly different ($P < 0.0001$). Thus, both ring and cytoplasmic α3 intensities are clearly higher in MSAs than in other afferents. The higher correlation for non-MSAs is mainly due to the lack of a ring of denser immunostaining, with ring and cytoplasmic staining being similar or the same. The poorer correlation for MSAs results from high α3 ring staining in all of them, but variable cytoplasmic staining. It suggests that the ring staining may be influenced weakly by cytoplamic α3 levels, but also by other factors.

α3 intensity in rat *versus* neuronal size. There was no correlation between α3 ring or cytoplasmic relative intensity and cell cross-sectional area (Fig. 4*B* and *C*). Thus, although α3 ring positive tend to be large, cell size

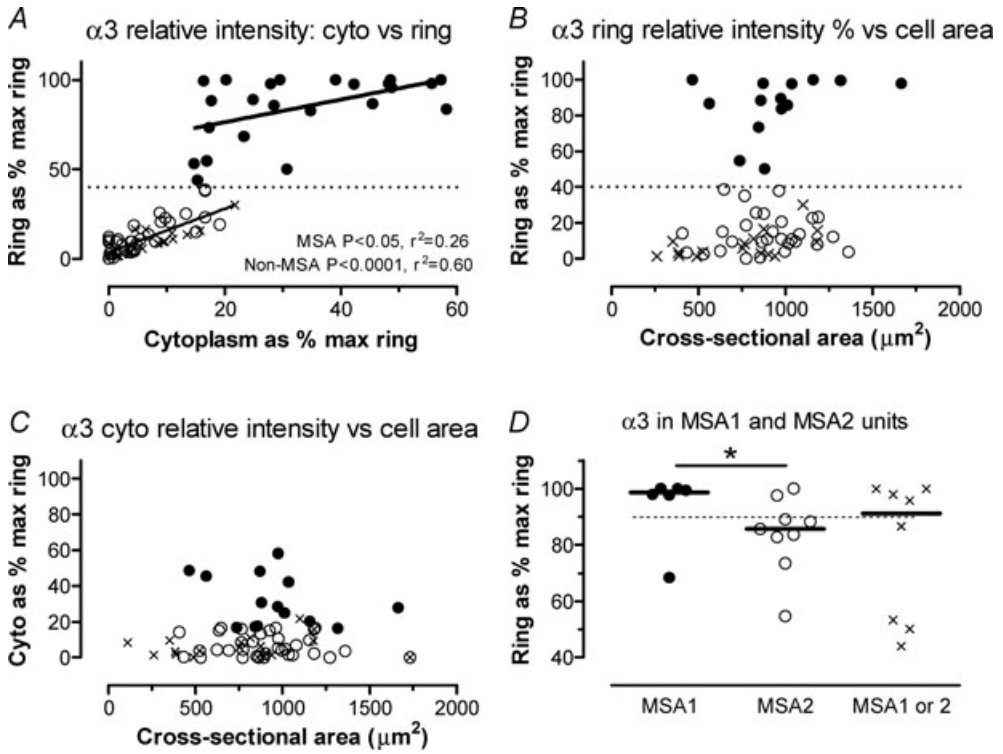

Figure 4. α3 ring staining in rat DRG *versus* cytoplasm, soma size and MSA subtype
A, plots of α3 cytoplasmic against α3 ring intensity (rat) show significant correlations both for MSAs and for all other units (of all CVs) together. These lines have significantly different slopes ($P < 0.0001$). *B* and *C*, size (largest cross-sectional area through each dye-injected neuron) was not correlated with α3 ring relative intensity (*B*) or cytoplasmic relative intensity (C). *D*, α3 ring staining in type I (MSA1), type II (MSA2) units and units incompletely characterised as either type. χ^2 test (Fisher's exact significance) shows significantly more MSA1 than MSA2 units with staining intensity >90% (the median for all 23 MSAs). Symbols in graphs *A*–*C*: filled circles, MSAs; open circles, all cutaneous (cut) LTMs; crosses, all nociceptors. In *D*, filled circles, MSA1 (type I); open circles, MSA2 (type II) and grey-filled circles indicate incompletely characterised units that could be MSA1 or MSA2. Asterisks denote level of significance as follows: $^*P < 0.05$, $^{**}P < 0.01$, $^{***}P < 0.001$.

per se appears not to be a determinant of α3 expression, underlining the relationship of α3 rings to MSA sensory properties and not to cell size.

α3 intensity in MSA1 and MSA2 units. The median conduction velocities of the MSA1 units was 24.2 m s^{-1}, while that for the MSA2 units was 12.3 m s^{-1}. Although not significantly different, this is consistent with the known properties of type I and type II MSAs. More MSA1 units had rings that were within the darkest three rings of the section. Relative intensities >100% were converted to 100%. A Mann–Whitney test between ring medians of MSA1 and MSA2 was non-significant. However, a χ test (Fisher's exact significance) of units below and above the median relative intensity for all 23 MSA units (90%) (see dotted line, Fig. 4*D*), was significant ($P < 0.05$). Thus, although MSA1, MSA2 and MSA units that were incompletely characterised as either, all had very high median α3 ring intensities, and significantly more MSA1 units had α3 rings with staining with a >90% relative intensity.

Discussion

The present study shows that neurons with high (clearly visible) α3 ring staining tend also to have high cytoplasmic α3 levels, and are likely to be MSAs. Identified MSAs had high α3 ring and cytoplasmic staining that was significantly higher than that in all other groups of identified neurons. This suggests that clear α3 ring immunoreactivity can be used to identify MSA DRG neurons, confirming predictions from immunohistochemical studies (Dobretsov *et al.* 2003).

The α3 ring staining was membrane related and not in satellite cells, and the correlation of ring with cytoplasmic intensities suggests the strong cytoplasmic and strong ring staining are within the same neurons. This location suggests that the α3 ring staining intensity might provide an indication of α3 levels within or very near the membrane, potentially performing Na^+ pump activity. The apparent thickness of the ring may have contributions from the known multiple projections and folding of the membrane of DRG neurons (Pannese *et al.* 1990) which in 7 μm sections could cause an apparent increase in width of the band of staining, and/or from possible accumulations of α3-stained vesicles just internal to the neuronal membrane.

We found high α3 immunostaining in MSAs in guinea pig as well as in rat DRGs. Similar staining in a subpopulation of large-diameter DRG neurons in amphibian, reptiles, birds and mammals (mouse and human) has previously been shown (Romanovsky *et al.* 2007). Thus, it seems that high expression of the α3 Na^+ pump isoform in MSAs is highly conserved in many species and across several phyla.

α3 as a marker for MSA neurons in DRGs

Although there are a number of useful markers of subsets of DRG neurons, a limited number have been examined in physiologically identified neurons and even fewer tied strongly to a particular sensory subtype. Any marker of functionally identified subdivisions of DRG neurons should be helpful in defining functional properties of normal neurons by immunostaining alone. So far, functional subdivisions have been defined immunocytochemically for all A-fibre neurons (neurofilament rich) (Lawson & Waddell, 1991); many nociceptors both those with C- and A-fibres express trkA, the high-affinity NGF receptor (Fang *et al.* 2005*a*); the peptides substance P and CGRP (Lawson *et al.* 1997 and 2002), and Nav1.8 (Djouhri *et al.* 2003) are expressed mainly in C- and A-fibre nociceptors. Only nociceptors express Nav1.9 (Fang *et al.* 2002) and many C-fibre nociceptors show binding for the lectin IB4 (Fang *et al.* 2006). For a review, see Lawson (2005). However, no clear label has previously been related directly to a subset of functionally identified low-threshold mechanoreceptive neurons. The clear immunostaining of MSAs by antibodies against the α3 subunit of the Na^+/K^+-ATPase will enable further useful subdivision of normal DRG neurons. For example, a question that it may help to answer is the identity of axotomised A-fibre neurons that show spontaneous firing, since these have been suggested to contribute to the onset of neuropathic pain (Amir *et al.* 1999; Liu *et al.* 2000; Sun *et al.* 2005). Lack of sensory endings makes their identity hard to determine. Use of α3 immunocytochemistry may exclude or identify these spontaneously firing neurons as MSAs, especially since our preliminary findings (L. Gao and S. N. Lawson, unpublished observations) show that despite a reduction in α3 staining intensity, similar proportions of neurons, with large diameters, show α3 rings from 1 to 7 days post axotomy. Thus, the α3 Na^+/K^+-ATPase ring staining may prove to be a useful addition to the available functionally characterised markers for DRG neurons. However, we did not provide any evidence relating to α3 in Golgi tendon organ afferent neurons, as the muscle relaxant would have made these hard to activate (see Methods).

These results raise several further questions, including whether the α3 ring staining is related to functionally active α3 Na^+/K^+-ATPase, and the mechanisms by which the α3 expression in the cytoplasm and ring might be controlled in DRG neurons. These issues remain to be addressed.

Although both type 1 and type 2 MSAs (MSA1 and MSA2) showed very high α3 ring staining, a higher proportion of type 1 units had maximum staining relative to other neurons in the same section. Although not the

case for all MSA1 units, there is a greater likelihood that neurons with the most intensely stained $\alpha 3$ rings in a section, are type 1 rather than type 2 MSAs.

Functional significance of $\alpha 3$ in MSAs

The $\alpha 1$ isoform of the Na^+ pump can restore ionic gradients across neuronal membranes with low activity/discharge rates (Blanco & Mercer, 1998). These are expressed in >80% DRG neurons (Dobretsov *et al.* 2003). However, in afferents with rapid or continuous firing, there is likely to be greater demand on Na^+ pump activity for restoration of Na^+ and K^+ concentration gradients. Compared with $\alpha 1$, the $\alpha 3$ pump has certain properties that may enable it better to meet this demand. These properties are a 2- to 3-fold higher threshold for activation by Na^+ and a slightly higher affinity for ATP (Jewell & Lingrel, 1991) and thus it is more likely that the intracellular Na^+ concentrations will increase to reach the Na^+ threshold for the $\alpha 3$ Na^+/K^+-ATPase in MSA neurons with periods of prolonged repetitive AP discharge. The higher affinity for ATP may facilitate this process. Overall, the properties of this $\alpha 3$ isoform of the Na^+/K^+-ATPase may be necessary to restore the normal Na^+ and K^+ gradients across the membrane in these highly active MSAs. Computer modelling and electrophysiological studies suggest that $\alpha 3$ Na^+/K^+-ATPase activity can increase the ability of CNS neurons to fire without accommodation (Sizov & Dobretsov, 2006; Kim *et al.* 2007). Thus, physiologically, higher $\alpha 3$ expression may enable MSAs to restore their membrane potentials during periods of rapid and/or prolonged tonic firing patterns, perhaps enabling this type of firing to be sustained for longer.

Conclusion

This study shows that the relative expression of the $\alpha 3$ subunit of the Na^+/K^+-ATPase is significantly higher in functionally identified MSAs than hindlimb cutaneous LTMs or nociceptive DRG neurons in rat and guinea pig. Of the neurons studied, MSAs consistently showed clear $\alpha 3$ ring staining. This therefore offers a selective immunostaining method for detecting MSAs *versus* other types of DRG neuron.

References

Amir R, Michaelis M & Devor M (1999). Membrane potential oscillations in dorsal root ganglion neurons: role in normal electrogenesis and neuropathic pain. *J Neurosci* **19**, 8589–8596.

Blanco G & Mercer RW (1998). Isozymes of the Na-K-ATPase: heterogeneity in structure, diversity in function. *Am J Physiol Renal Physiol* **275**, F633–F650.

Boyd IA (1962). Structure and innervation of nuclear bag muscle fibre system and nuclear chain muscle fibre system in mammalian muscle spindles. *Philos Trans R Soc Lond Ser B Biol Sci* **245**, 81–136.

Brown MC, Engberg I & Matthews PB (1967). The relative sensitivity to vibration of muscle receptors of the cat. *J Physiol* **192**, 773–800.

Calvert R & Anderton BH (1982). *In vivo* metabolism of mammalian neurofilament polypeptides in developing and adult rat brain. *FEBS Lett* **145**, 171–175.

Chaplan SR, Guo HQ, Lee DH, Luo L, Liu C, Kuei C, Velumian AA, Butler MP, Brown SM & Dubin AE (2003). Neuronal hyperpolarization-activated pacemaker channels drive neuropathic pain. *J Neurosci* **23**, 1169–1178.

Charlemagne D, Mayoux E, Poyard M, Oliviero P & Geering K (1987). Identification of two isoforms of the catalytic subunit of Na,K-ATPase in myocytes from adult rat heart. *J Biol Chem* **262**, 8941–8943.

Clausen T (2003). Na^+-K^+ pump regulation and skeletal muscle contractility. *Physiol Rev* **83**, 1269–1324.

Djouhri L, Bleazard L & Lawson SN (1998). Association of somatic action potential shape with sensory receptive properties in guinea-pig dorsal root ganglion neurones. *J Physiol* **513**, 857–872.

Djouhri L, Fang X, Okuse K, Wood JN, Berry CM & Lawson S (2003). The TTX-resistant sodium channel $Na_v1.8$ (SNS/PN3): expression and correlation with membrane properties in rat nociceptive primary afferent neurons. *J Physiol* **550**, 739–752.

Djouhri L & Lawson SN (2001). Increased conduction velocity of nociceptive primary afferent neurons during unilateral hindlimb inflammation in the anaesthetised guinea-pig. *Neuroscience* **102**, 669–679.

Dobretsov M, Hastings SL, Sims TJ, Stimers JR & Romanovsky D (2003). Stretch receptor-associated expression of α_3 isoform of the Na^+,K^+-ATPase in rat peripheral nervous system. *Neuroscience* **116**, 1069–1080.

Dobretsov M, Hastings SL & Stimers JR (1999). Non-uniform expression of α subunit isoforms of the Na^+/K^+ pump in rat dorsal root ganglia neurons. *Brain Res* **821**, 212–217.

Drummond GB (2009). Reporting ethical matters in *The Journal of Physiology*: standards and advice. *J Physiol* **587**, 713–719.

Fang X, Djouhri L, Black JA, Dib-Hajj SD, Waxman SG & Lawson SN (2002). The presence and role of the tetrodotoxin-resistant sodium channel $Na_v1.9$ (NaN) in nociceptive primary afferent neurons. *J Neurosci* **22**, 7425–7433.

Fang X, Djouhri L, McMullan S, Berry C, Okuse K, Waxman SG & Lawson SN (2005*a*) TrkA is expressed in nociceptive neurons and influences electrophysiological properties via $Na_v1.8$ expression in rapidly conducting nociceptors. *J Neurosci* **25**, 4868–4878.

Fang X, Djouhri L, McMullan S, Berry C, Waxman SG, Okuse K & Lawson SN (2006). Intense isolectin-B4 binding in rat dorsal root ganglion neurons distinguishes C-fiber nociceptors with broad action potentials and high Nav1.9 expression. *J Neurosci* **26**, 7281–7292.

Fang X, McMullan S, Lawson SN & Djouhri L (2005*b*). Electrophysiological differences between nociceptive and non-nociceptive dorsal root ganglion neurones in the rat *in vivo*. *J Phyiol* **565**, 927–943.

Han W, Bao W, Wang Z & Nattel S (2002). Comparison of ion-channel subunit expression in canine cardiac Purkinje fibers and ventricular muscle. *Circ Res* **91**, 790–797.

Jewell EA & Lingrel JB (1991). Comparison of the substrate dependence properties of the rat Na,K-ATPase α1, α2, and α3 isoforms expressed in HeLa cells. *J Biol Chem* **266**, 16925–16930.

Juhaszova M & Blaustein MP (1997). Na^+ pump low and high ouabain affinity α subunit isoforms are differently distributed in cells. *Proc Natl Acad Sci U S A* **94**, 1800–1805.

Kim JH, Sizov I, Dobretsov M & von Gersdorff H (2007). Presynaptic Ca^{2+} buffers control the strength of a fast post-tetanic hyperpolarization mediated by the α3 Na^+/K^+-ATPase. *Nat Neurosci* **10**, 196–205.

Lawson SN (2005). The peripheral sensory nervous system: dorsal root ganglion neurons. In *Peripheral Neuropathy*, eds Dyck PJ & Thomas PK, pp. 163–202. W.B. Saunders; Elsevier, Inc.

Lawson SN, Crepps BA & Perl ER (1997). Relationship of substance P to afferent characteristics of dorsal root ganglion neurones in guinea-pig. *J Physiol* **505**, 177–191.

Lawson SN, Harper AA, Harper EI, Garson JA & Anderton BH (1984). A monoclonal antibody against neurofilament protein specifically labels a subpopulation of rat sensory neurones. *J Comp Neurol* **228**, 263–272.

Lawson SN & Waddell PJ (1991). Soma neurofilament immunoreactivity is related to cell size and fibre conduction velocity in rat primary sensory neurons. *J Physiol* **435**, 41–63.

Lawson SN, Crepps B, Perl ER (2002). Calcitonin gene-related peptide immunoreactivity and afferent receptive properties of dorsal root ganglion neurones in guinea-pigs. *J Physiol* **2002**, 989–1002.

Liu CN, Michaelis M, Amir R & Devor M (2000). Spinal nerve injury enhances subthreshold membrane potential oscillations in DRG neurons: relation to neuropathic pain. *J Neurophysiol* **84**, 205–215.

McDonough AA, Geering K & Farley RA (1990). The sodium pump needs its β subunit. *FASEB J* **4**, 1598–1605.

Mata M, Siegel GJ, Hieber V, Beaty MW & Fink DJ (1991). Differential distribution of (Na,K)-ATPase α isoform mRNAs in the peripheral nervous system. *Brain Res* **546**, 47–54.

Matthews PBC (1964). Muscle spindles and their motor control. *Physiol Rev* **44**, 219–288.

Matthews PBC (1984). Evidence from the use of vibration that the human long-latency stretch reflex depends upon spindle secondary afferents. *J Physiol* **348**, 383–415.

Much B, Wahl-Schott C, Zong X, Schneider A, Baumann L, Moosmang S, Ludwig A & Biel M (2003). Role of subunit heteromerization and N-linked glycosylation in the formation of functional hyperpolarization-activated cyclic nucleotide-gated channels. *J Biol Chem* **278**, 43781–43786.

Notomi T & Shigemoto R (2004). Immunohistochemical localization of Ih channel subunits, HCN1-4, in the rat brain. *J Comp Neurol* **471**, 241–276.

Pannese E, Ledda M, Conte V, Procacci P & Matsuda S (1990). Scanning electron-microscope observations of the perikaryal projections of rabbit spinal ganglion neurons after enzymatic removal of connective tissue and satellite cells. *Cell Tissue Res* **260**, 167–173.

Peters CJ, Chow SS, Angoli D, Nazzari H, Cayabyab FS, Morshedian A & Accili EA (2009). In situ co-distribution and functional interactions of SAP97 with sinoatrial isoforms of HCN channels. *J Mol Cell Cardiol* **46**, 636–643.

Pressley TA (1992). Phylogenetic conservation of isoform-specific regions within alpha-subunit of Na^+-K^+-ATPase. *Am J Physiol Cell Physiol* **262**, C743–C751.

Romanovsky D, Moseley AE, Mrak RE, Taylor MD & Dobretsov M (2007). Phylogenetic preservation of α3 Na^+,K^+-ATPase distribution in vertebrate peripheral nervous systems. *J Comp Neurol* **500**, 1106–1116.

Rosenthal M & Sick TJ (1992). Glycolytic and oxidative metabolic contributions to potassium ion transport in rat cerebral cortex. *Can J Physiol Pharmacol* **70**, S165–S169.

Sizov I & Dobretsov M (2006). Sodium affinity of the Na,K-ATPase and reliability of afferent signaling. *2006 Abstract Viewer/Itinerary Planner*, Programme No. 729.5. Society for Neuroscience, Washington, DC.

Sun Q, Tu H, Xing GG, Han JS & Wan Y (2005). Ectopic discharges from injured nerve fibers are highly correlated with tactile allodynia only in early, but not late, stage in rats with spinal nerve ligation. *Exp Neurol* **191**, 128–136.

Sweadner KJ (1989). Isozymes of the Na^+/K^+-ATPase. *Biochim Biophys Acta* **988**, 185–220.

Waddell PJ, Lawson SN & McCarthy PW (1989). Conduction velocity changes along the processes of rat primary sensory neurons. *Neuroscience* **30**, 577–584.

Wood JW & Anderton BH (1981). Monoclonal antibodies to mammalian neurofilaments. *Biosci Rep* **1**, 263–268.

Acknowledgements

Supported by a Wellcome trust grant to S.N.L. Thanks to Thomas Pressley for the anti-α3 antibody, to K. W. Ranatunga, T. J. Biscoe, T. Clausen and R. M. A. P. Ridge for discussions and comments.

Author's present addresses

A. Parekh: Poole Hospital NHS Foundation Trust, Longfleet Road, Dorset, BH15 2JB, UK.

L. Djouhri: Department of Pharmacology & Therapeutics, University of Liverpool, Liverpool L69 3GE, UK.

X. Fang: Neurosolutions Ltd and Department of Biological Sciences, University of Warwick, CV4 7AL, UK.

S. McMullan: Australian School of Advanced Medicine, Macquarie University, Sydney 2109, Australia.